Journal of The Electrochemical Society, **149** (8) A1008-A1014 (2002)
0013-4651/2002/149(8)/A1008/7/$7.00 © The Electrochemical Society, Inc.

Nitric Acid Modification of Activated Carbon Electrodes for Improvement of Electrochemical Capacitance

Yau-Ren Nian and Hsisheng Teng*,z

Department of Chemical Engineering, National Cheng Kung University, Tainan 70101, Taiwan

Nitric acid oxidation of activated carbon fabric in combination with calcination in N_2 at different temperatures was conducted to explore the influence of surface carbon-oxygen complexes on the performance of electrochemical capacitors fabricated with the carbon fabric. The performance of the capacitors was tested in 1 M H_2SO_4 within a potential range of −0.6 and 0.6 V. The specific capacitance of the carbon was found to increase upon oxidation. Surface complex analysis using temperature programmed desorption showed that the double-layer capacitance was enhanced due to the presence of CO-desorbing complexes while CO_2-desorbing complexes exhibited a negative effect. The micropore resistance for ion migration was low for these carbons. The electrical connection resistance between the fabric and the backing plate as well as that between the carbon fibers accounted for the major proportion of the overall resistance and was shown to increase due to oxidation. A capacitance increase of more than 40% has been achieved, without increasing IR drop, by nitric acid oxidation followed by 450°C calcination that was shown to remove the majority of the CO_2-desorbing complexes while retaining the CO-desorbing complexes.
 [DOI: 10.1149/1.1490535]

Manuscript submitted October 31, 2001; revised manuscript received February 11, 2002. Available electronically June 21, 2002.

Because of the high energy storage capability, electrochemical capacitors (ECs), which still retain the high power density feature of conventional capacitors, have received considerable attention for serving as peak-power or backup energy sources.[1-4] Porous carbon is the electrode material used most frequently for ECs. Use of high surface-area carbon electrodes results in large capacitance, mainly due to the formation of the double layer at the electrode surface.[5-7] In addition to the charge accumulation mechanism that forms the double layer on the carbon surface, there are possible contributions from hetero-atom surface complexes that would provide sites for reversible chemisorption of a working ion and thus give rise to pseudocapacitance.[8-12]

The presence of oxygen surface complexes on carbon electrodes of an EC has been shown to affect the performance of the capacitor.[13-16] In acidic solutions, increasing the population of oxygen surface complexes generally results in an increase of the double-layer capacitance. The capacitance increase can be partially ascribed to the specific adsorption of ions and solvent molecules, which is caused by the enhanced affinity toward protons due to the electronic density change in the neighborhood of surface complexes.[14,17] Some types of oxygen functional groups may provide redox activity to enhance the pseudocapacitance.[16]

Oxygen functional groups can be formed on carbon surfaces when they are treated with oxidizing gases, such as O_2,[17] or oxidizing acid solutions, such as nitric acid.[18,19] Various types of oxygen functional groups are formed from these treatments, and the distribution of these groups varies with the types of the oxidizing agents.[20] It has been reported that carbons with different complexes have different effects in adsorption or catalysis.[21] The roles that different functional groups play in the formation of electric double layers have not yet been clearly elucidated. In the present work, activated carbon fabrics modified using nitric acid oxidation combined with thermal treatment are prepared. The chemical compositions of the introduced surface oxides in these porous carbons are characterized using the thermal desorption technique, and the electrochemical performances of the resulting capacitors are also examined, in an attempt to identify the effects of different oxygen groups on double-layer formation.

Experimental

Oxidation of activated carbon.—Polyacrylonitrile (PAN)-based activated carbon fabric supplied by Taiwan Carbon Technology, Co., Taiwan, was employed as the basic electrode material for the capacitors in the present work. The fabric has a thickness of 0.4-0.6 mm. To avoid any intrusion of unexpected influence of retained surface oxides, the carbon fabric was cleaned by calcination at 900°C in N_2 for 20 min prior to any measurement or further treatment. The thermally treated carbon fabric (CFT) served as the fresh carbon in the present work.

Nitric acid was used in the oxidation treatment of CFT. The treatment was initiated by stirring 1 g of the carbon in a 2 N nitric acid solution. The stirring was performed at 90°C for 1 h. After nitric acid treatment, the treated sample was then leached by mixing with 250 mL of distilled water, followed by filtration of the mixtures. Leaching was carried out several times until the pH value of the water-carbon mixture was above 6. The leached product was then dried in vacuum at 110°C for 7 h, to give the nitric acid-oxidized fabric. To prepare carbons containing different populations of surface complexes, the oxidized fabric was subjected to calcination at temperatures of 150, 300, 450, 600, and 750°C under N_2 flow for 1 h.

Surface characterization of the carbon samples.—Specific surface areas and pore volumes of the carbon fabric were determined by N_2 gas adsorption at −196°C. An automated adsorption apparatus (Micromeritics ASAP 2010, USA) was employed for these measurements. Surface areas and micropore volumes of the samples were evaluated with the application of the Brunauer-Emmett-Teller (BET) and Dubinin-Radushkevich (DR) equations,[22] respectively. The amount of N_2 adsorbed at relative pressures near unity was employed to determine the total pore volume, which corresponds to the sum of the micropore and mesopore volumes.[23]

The temperature programmed desorption (TPD) technique was employed to analyze the population of carbon-oxygen complexes on the fabric samples. The measurements were conducted under a helium flow, by heating 0.05 g of a sample from room temperature to 950°C at a linear heating rate of 30°C min^{-1}. The evolution of CO and CO_2 during TPD was continuously monitored using a nondispersive infrared analyzer.

Electrochemical measurements.—Sandwich-type cells were prepared to examine the electrochemical performance of the carbon fabric samples. The electrodes of the cells consisted of 2 cm^2 fabrics and stainless-steel-foil current collectors. The cells were constructed with a pair of the electrodes and a piece of filter paper as the separator. All electrochemical measurements were carried out at ambient temperature using 1 M H_2SO_4 as electrolyte. For potential-sweep cyclic voltammetric measurements, the potential scan rate ranged form 0.5 to 3 mV s^{-1} within a potential range of −0.6 to 0.6 V. The

* Electrochemical Society Active Member.
z E-mail: hteng@mail.ncku.edu.tw

Table I. Physical characteristics of the carbon fabric samples obtained from different treatment processes.

Carbon sample	Calcination temp. (°C)	Surf. area (m^2 g^{-1})	Pore volume (cm^3 g^{-1})	Pore size distribution	
				micro (%)	meso (%)
CFN150	150	925	0.44	100	0
CFN300	300	1030	0.49	100	0
CFN450	450	1080	0.52	100	0
CFN600	600	1140	0.55	100	0
CFN750	750	1060	0.51	98	2
CFT[a]	900	1170	0.56	100	0

[a] No nitric acid oxidation executed prior to thermal treatment.

capacitance of the electrodes was measured by charging the cells at 0.5 mA to 0.6 V, followed by discharging to 0 V at different currents of 0.5, 1, 2, and 3 mA.

An ac impedance spectrum analyzer combined with computer software was employed to measure and analyze the ac impedance behavior of the capacitors. In this work, the potential amplitude of ac was equal to 5 mV, and the frequency range was from 10 mHz to 100 kHz at 0 V.

Results and Discussion

Surface characteristics of the carbon samples.—The physical characteristics of the carbon samples determined from N_2 adsorption are given in Table I. These carbon samples were designated using the nomenclature of the carbon fabric treated with nitric acid, CFN, followed by the calcination temperature. The data show that the pore volumes of these samples are predominantly contributed by micropores. Both the surface area and pore volume decrease due to the oxidation treatment with nitric acid, indicating that the introduction of the surface oxides has hindered the access of N_2 into the carbon micropores. Upon calcination in N_2 to remove the hindering oxides, a slight porosity increase of the oxidized samples can be observed. Nevertheless, the influence of physical characteristics is considered to be minor in this work, since the changes in porosity and pore size distribution caused by the treatment are not obvious.

The population of oxygen functional groups present on the carbon surface was evaluated using TPD. It has been well known that upon thermal treatment in an inert environment, oxygen functional groups such as carboxyl, anhydride, and lactone groups would desorb as CO_2 while hydroxyl, carbonyl, and quinone groups would desorb as CO.[13,20,24] Figure 1 shows examples of the CO_2 and CO evolution profiles during TPD of CFN150, CFN450, and CFN750. It can be seen from the CFN150 spectra that CO_2 evolution occurs mainly at low temperatures and it is split into two lumps centered at 330 and 600°C. The evolution of CO occurs mainly at temperatures higher than 600°C. Upon calcination to 450°C, the low temperature CO_2-desorbing complexes diminish, while the CO evolution shows a slight increase. The calcination at 750°C removed almost all the CO_2-desorbing complexes and the majority of the CO-desorbing ones.

The accumulated amounts of CO_2 and CO evolutions during TPD are given in Table II. The results show that the amount of CO_2 evolved from these carbon samples decreases with increasing calcination temperature, while that of CO evolved increases slightly with the temperature and passes through a maximum at 450°C before showing a decreasing trend. The total O evolution calculated from the amounts of CO_2 and CO decreases monotonically with the calcination temperature. The decrease in the amounts of CO_2- and CO-desorbing complexes with the calcination temperature is expected, since the oxidized sites would undergo decomposition and become vacant upon calcination. The increase in CO-desorbing complexes in the low calcination temperature regime is not expected. This probably results from the transformation of some CO_2-desorbing complexes into CO-desorbing during the period of calcination.

Electrochemical performance of the resulting capacitors.—To illustrate the influence of the surface oxides on the capacitance of carbon fabric samples, constant current charge-discharge cycling was conducted to measure the capacitance of the resulting capacitor cells. The specific discharge capacitance of the electrodes in the cells was calculated according to

$$C = (2 \times I \times t)/(W \times \Delta E)$$

where I is the discharge current, t the discharge time, W the carbon fabric mass on an electrode, and ΔE the potential difference in discharge, excluding the portion of IR drop. The factor of 2 comes from the total capacitance measured from the test cells being the addition of two equivalent single-electrode capacitors in series.

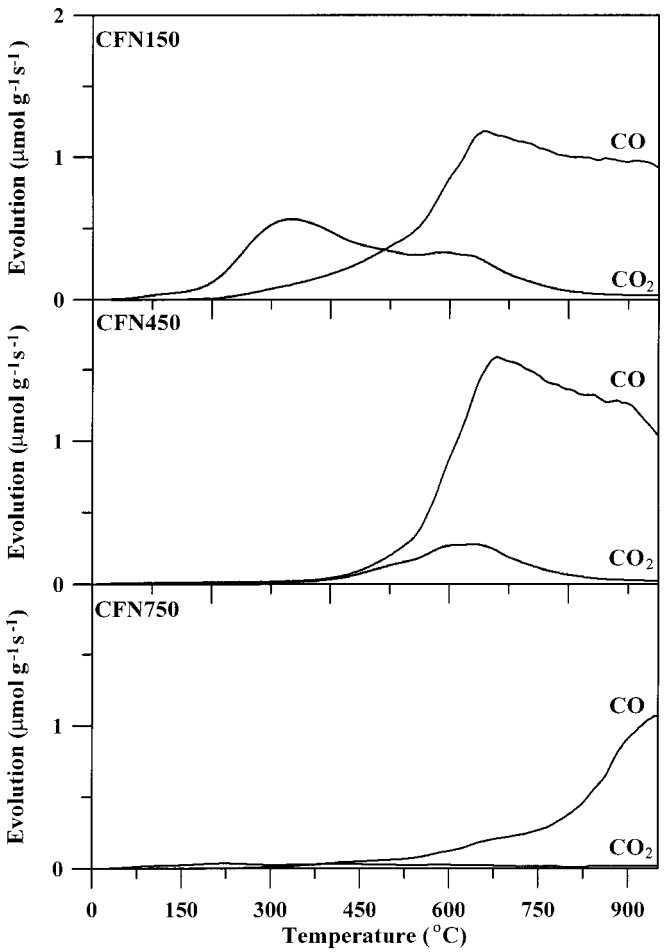

Figure 1. Evolution profiles of CO_2 and CO by temperature programmed desorption for different carbon fabrics.

Table II. Accumulated amounts of CO_2, CO, and total O evolutions from the carbon fabrics during temperature programmed desorption.

Carbon type	CO_2 evolution (mmol g^{-1})	CO evolution (mmol g^{-1})	Total O evolution (mmol g^{-1})
CFN150	0.21	0.46	0.88
CFN300	0.14	0.52	0.80
CFN450	0.07	0.53	0.67
CFN600	0.03	0.35	0.41
CFN750	0.03	0.17	0.23
CFT	0.03	0.08	0.14

Figure 2 shows the specific capacitances of the samples calcined at different temperatures. For each sample the capacitance decreases with discharge current, suggesting the existence of ohmic resistance for electrolyte migration in the axial direction of micropores. However, the resistance must be rather small since the capacitance decrease is not obvious. This may be due to the small depth of micropores in the carbon fibers. As to the effect of oxidation, the results reflect that the specific capacitance of the carbon fabric increases upon nitric acid treatment, except that CFN750 has capacitances slightly lower than those of CFT. The extent of calcination in N_2 following the oxidation shows a great influence on the performance of the resulting cells. The capacitance increases with the calcination temperature and reaches a maximum value at a temperature of 450°C before decreasing with further increases in the temperature. Obviously, not only the population but also the type of surface oxides affects the capacitance.

Comparing the specific capacitance and the accumulated amount of CO-desorbing complexes of the samples, both quantities show similar variation trends with the calcination temperature and both have a maximum value at 450°C. This indicates that the electrochemical capacitance of carbon can be improved through the introduction of CO-desorbing complexes, such as carbonyl and quinone.[8,9] However, the variation of capacitance was not solely determined by the amount of CO-desorbing complexes. For example, CFN150 has a larger amount of CO-desorbing complexes than CFN600, but has a lower capacitance. Furthermore, the slight

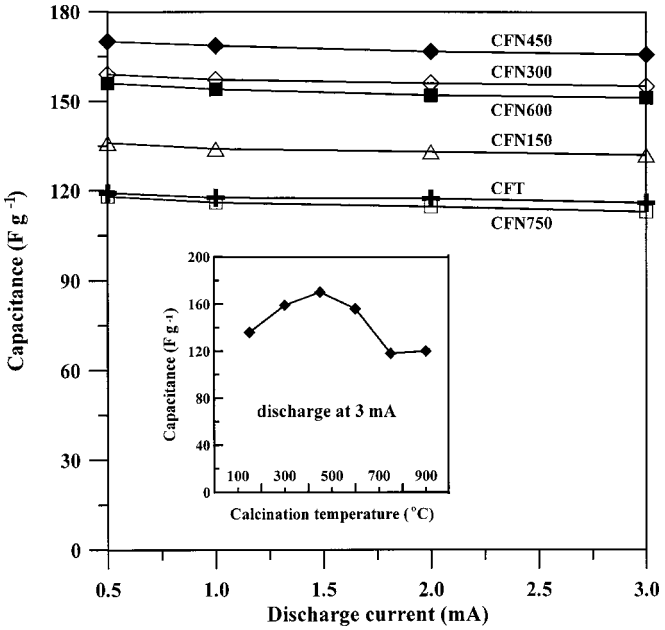

Figure 2. Variation of specific discharge capacitance with the discharge current for different electrodes (2 cm^2) charged at 0.5 mA to 0.6 V. An example of the capacitance *vs.* the calcination temperature is also provided.

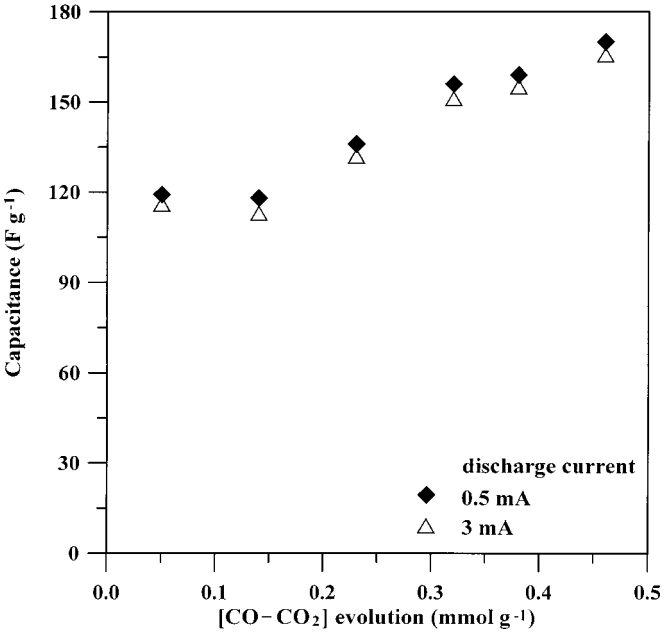

Figure 3. Variation of specific capacitance with the difference of CO evolution minus CO_2 evolution ([CO - CO_2]) in TPD.

increase in the amount of CO-desorbing complexes with temperature for calcination temperatures lower than 450°C cannot explain the sharp increase in capacitance with the temperature. On the other hand, the amount of CO_2-desorbing complexes shows a rapid decreasing trend within this temperature range. This indicates that CO_2-desorbing complexes might play an inhibitor role in this energy storage process.

The effects of the CO- and CO_2-desorbing complexes on the charge-discharge mechanism can be further illustrated by plotting the capacitance against the difference of CO evolution minus CO_2 evolution. The results are shown in Fig. 3, showing that the capacitance is an increasing function of the difference between the amounts of the two types of complexes. This has demonstrated that the positive and the negative roles that the CO- and the CO_2-desorbing complexes, respectively, act to improve the capacitance. On the basis of the preceding results, one can conclude that a more than 40% capacitance increase can be achieved through nitric acid oxidation in combination with 450°C thermal treatment that would remove the majority of CO_2-desorbing complexes while leaving the CO-desorbing unchanged.

The IR drop, a sudden potential drop at the very beginning of discharge, was measured and plotted against the discharge current in Fig. 4. This potential drop results mainly from the electrical connection resistance, bulk solution resistance, and resistance of ion migration in carbon micropores.[25,26] Figure 4 shows that the IR drop increases linearly with the current, and the slope of this linear relationship can be used to calculate the overall resistance of the electrodes. The calculated values are listed in Table III, showing that the resistance variation with the calcination temperature can be divided into two temperature regimes. For temperatures lower than 450°C, the resistance decreases with the temperature and reaches a minimum of 23 Ω at 450°C. In the high temperature regime (>450°C), the resistance also shows a decreasing trend with temperature. The variation of the resistance may relate to the formation of water aggregates around the complexes,[27,28] carbon wettability,[13] and the area for electrical connection of the fibers.[15] This aspect is discussed in combination with the results from ac impedance measurements.

Potential sweep cyclic voltammetric measurements were conducted within a potential range of −0.6 to 0.6 V to analyze the electrochemical behavior of the capacitors. Figure 5a shows the vol-

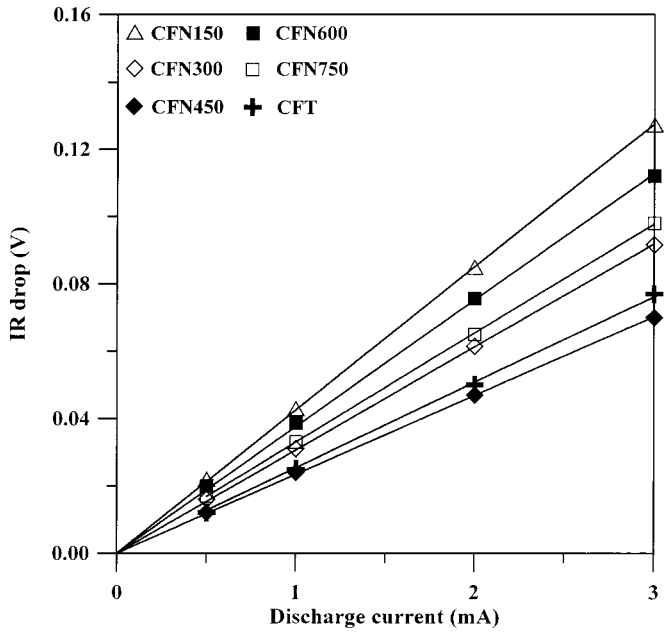

Figure 4. Variation of IR drop with the discharge current for different electrodes (2 cm^2) charged at 0.5 mA to 0.6 V.

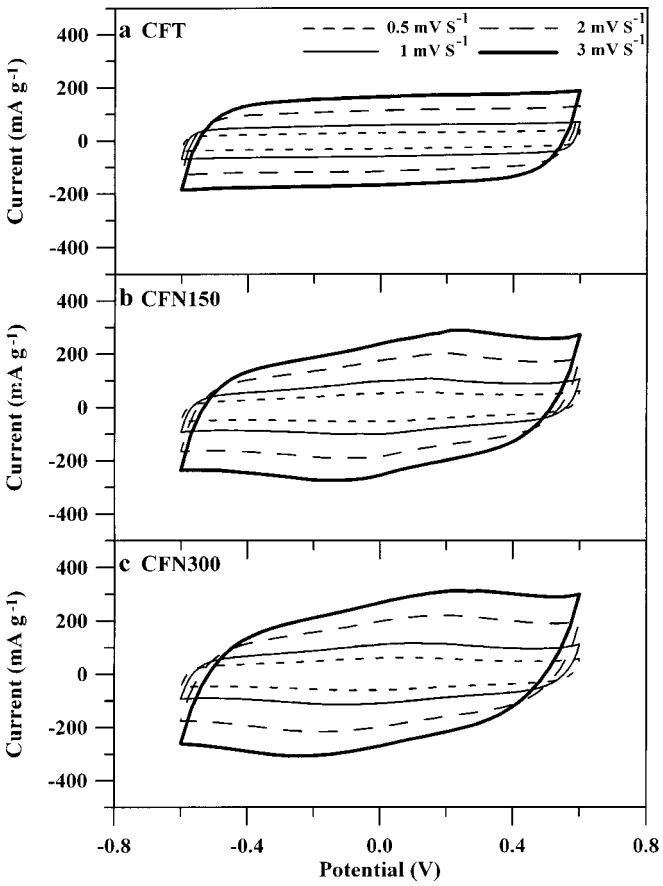

Figure 5. Cyclic voltammograms of the (a) CFT, (b) CFN150, and (c) CFN300 electrodes (2 cm^2) in 1 M H_2SO_4 at different potential sweep rates.

tammograms of the CFT capacitor with different potential sweep rates. Rectangular voltammograms were obtained, indicating the domination of double-layer formation in the energy storage process. The resistance for ion migration in micropores was seen to be present in this system, since increasing the sweep rate aggravated the delay of the current to reach a horizontal value after reversal of the potential sweep.[29-31] The resistance would combine with the existence of the distributed capacitance to delay the current inversion.

The voltammograms of the CFN150 capacitor are shown in Fig. 5b. In comparison with CFT, CFN150 not only gives a higher background current in the potential sweep, indicating a higher double-layer capacitance, but also exhibits faradaic peak currents in the voltammograms. The voltammograms of the CFN300 capacitor, which are shown in Fig. 5c, are similar to those of the CFN150 in shape, but exhibit higher current values because of the higher capacitance that has been presented in Fig. 2. The voltammograms of the CFN450, CFN600, and CFN750 capacitors are shown in Fig. 6, showing that no obvious faradaic current can be observed. This may be related to the low population of the CO_2-desorbing complexes of these carbon samples.

In the voltammograms, both the anodic and cathodic currents, I_a and I_c, respectively, are increasing functions of the potential sweep rate. The difference of the two opposite currents at 0 V, $\Delta I(= I_a - I_c)$, was calculated and plotted against the sweep rate. From the linear relationship in the plot, the total capacitance (C_t) associated with double-layer formation and potential-dependent redox processes within the potential-sweep rate range at 0 V can be estimated from the slope.[32] The data of C_t are listed in Table III. The values of C_t are similar to those obtained from the charge-discharge cycling measurements shown in Fig. 2. Still, C_t was shown to increase upon oxidation, and its maximum value occurred at a calcination temperature of 450°C. The results again reflect the positive role of the CO-desorbing complexes, *i.e.*, the carbonyl- or quinone-type groups, in capacitance enhancement. With the presence of these groups, an equilibrium reaction may occur in the carbon electrode[14]

$$>C_xO + H^+ = >C_xO\|H^+ \quad [1]$$

where $>C_xO\|H^+$ represents a proton adsorbed by a carbonyl- or quinone-type site. This specific adsorption process may facilitate an excess specific double-layer capacitance due to the local changes of electronic charge density. Because no obvious peaks are observed in the cyclic voltammograms of the CFN450 and CFN600 capacitors, it is suggested that the increase of capacitance upon oxidation arises mainly from the enhanced affinity toward protons in an acid solution.

Obvious faradaic peak currents are observed for carbon electrodes with high oxygen contents. The results imply that both the CO- and CO_2-desorbing complexes may be involved in the electron transfer mechanisms that result in the faradaic currents. Apart from Eq. 1, a redox mechanism for a carbonyl or quinone-type group has been proposed[16]

$$>C_xO + H^+ + e^- = >C_xOH \quad [2]$$

where $>C_xOH$ represents a phenol- or hydroquinone-type complex and e^- an electron. This reaction should make a partial contribution to the pseudocapacitance of the oxidized electrodes. The functions

Table III. Overall resistance of different capacitors determined from IR drop and total capacitance determined from potential-sweep cyclic voltammograms.

Carbon type	Overall resistance (Ω)	C_t (F g^{-1})
CFN150	43	135
CFN300	31	159
CFN450	23	170
CFN600	38	154
CFN750	33	111
CFT	26	110

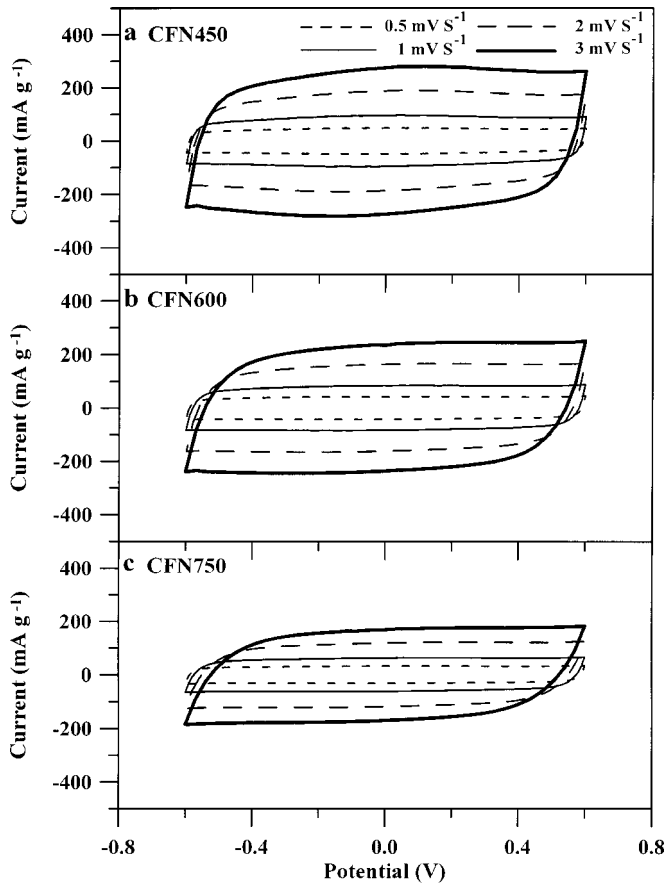

Figure 6. Cyclic voltammograms of the (a) CFN450, (b) CFN600, and (c) CFN750 electrodes (2 cm^2) in 1 M H_2SO_4 at different potential sweep rates.

of CO_2-desorbing complexes in promoting the faradaic currents may be significant, but have never been interpreted in the literature. This aspect will be the subject of additional research.

The technique of ac impedance spectroscopy was further employed to analyze the electrochemical behavior of the capacitors. The impedance spectra of the different capacitors are shown as Nyquist plots in Fig. 7. A single semicircle can be observed in the high-frequency region for all the capacitors. The plots are transformed to a vertical line in the $-\mathrm{Im}(Z)$ direction with decreasing frequency. Accordingly, the equivalent circuit for the carbon electrodes should involve the following circuit elements: the bulk solution resistance, R_s; the double layer capacitance, C_{dl}; a faradaic resistance, R_F, corresponding to the reciprocal of the potential-dependent charge-transfer rate in reactions like Eq. 2; a pseudocapacitance, C_p, associated with the potential dependence of the redox-site concentration in Eq. 2; and C_c and R_c due to the impedence between the fibers as well as that between the fabric and the backing plate for the electrical connection. The combination of the circuit elements is proposed and shown in Fig. 8. The faradaic resistance, R_F, should be very large, since there is no second semicircle observed in the plots. This may be due to the inert nature of the carbon surface.

The overall impedance, Z, of the equivalent circuit in Fig. 8 is given by

$$Z = R_s + \frac{R_c}{j\omega R_c C_c + 1} + \frac{1}{j\omega C_{dl} + \dfrac{j\omega C_p}{j\omega R_F C_p + 1}} \qquad [3]$$

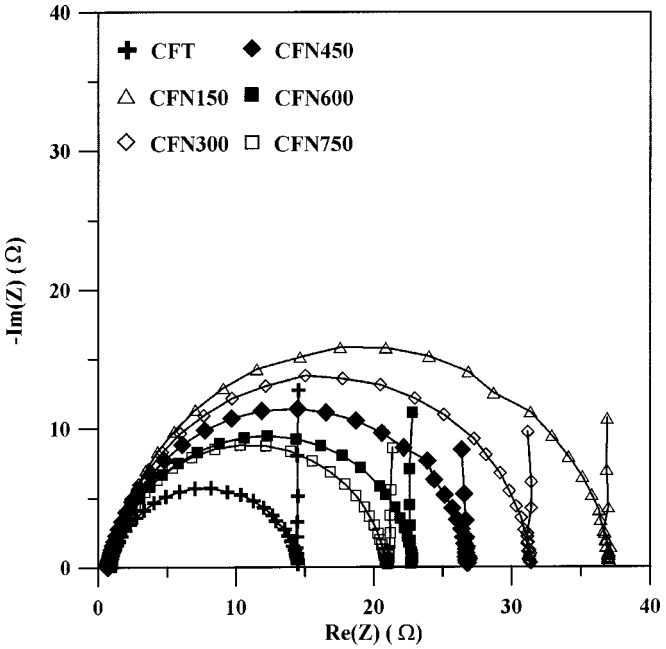

Figure 7. Nyquist impedance plots of different electrodes in 1 M H_2SO_4 with frequency ranging from 10 mHz to 100 kHz at 0 V.

From the above equation it can be seen that two limiting cases, low- and high-frequency regions, arise. The vertical alignment of impedance plots in the low-frequency region suggests the capacitive behavior. With the frequency approaching zero and the high value of R_F, Eq. 3 can be reduced to

$$Z = R_s + R_c - j/\omega(C_{dl} + C_p) \qquad [4]$$

The intercept on the Re(Z) axis is $R_s + R_c$, while $-\mathrm{Im}(Z) = 1/\omega(C_{dl} + C_p)$ can be used to estimate the overall capacitance of the electrode. At sufficiently high frequencies, the overall impedance can be transformed to

$$Z = R_s + \frac{R_c}{j\omega R_c C_c + 1} \qquad [5]$$

The above equation would correspond to a locus showing a semicircle that intercepts the Re(Z) axis at R_s and $R_s + R_c$ in the Nyquist plot.

Equations 4 and 5 together with the impedance data in Fig. 7 were employed to estimate the values of the elements of the equivalent circuit in Fig. 8. The estimated values are summarized in Table IV. The bulk solution resistance was found to be small and showed little variation with the population of surface oxides. The overall capacitance, $C_{dl} + C_p$, obtained from Eq. 4 is similar to that determined using cyclic voltammetry as well as that from charge-discharge cycling. Still, the CFN450 electrode gives the highest ca-

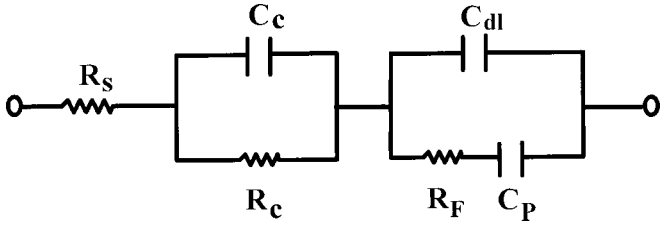

Figure 8. Equivalent circuit for the impedance spectra of the carbon fabric electrodes.

Table IV. Components of the equivalent circuit fitted for the impedance spectra.

Carbon type	R_s (Ω)	R_c (Ω)	C_c ($\mu F\ g^{-1}$)	$C_{dl} + C_p$ ($F\ g^{-1}$)
CFN150	0.8	35	27	125
CFN300	0.8	30	26	139
CFN450	0.7	25	26	160
CFN600	0.7	23	27	138
CFN750	0.7	21	28	129
CFT	0.8	14	36	118

pacitance. The value of C_c was negligibly small compared to the overall capacitance. However, the value of R_c was considerably higher and could account for a major proportion of the overall resistance estimated from the IR drop, which has been stated to result mainly from the electrical connection resistance (R_c), bulk solution resistance (R_s), and resistance of ion migration in carbon micropores. This R_c value was found to increase with the population of surface oxides, indicating the reduction of the area of the electrical connection due to the introduction of the oxides.

Because of the small values of R_s, the overall resistance can be considered to be the sum of R_c and the resistance for ion migration in micropores. Interestingly enough, the CFN450 capacitor exhibited an R_c value about the same as the overall resistance. This implies a negligibly small resistance for ion migration in the micropores of CFN450. The cyclic voltammograms of CFN450 in Fig. 6a, that show a quick current reversal after changing the potential sweep direction, can support this interpretation. For carbons with calcination temperatures lower than 450°C, the difference of the overall resistance minus R_c decreases with the temperature. This suggests that increasing the population of surface oxides would retard ion migration due to formation of water aggregates and thus increase the resistance in micropores. As for carbons that have been calcined to higher temperatures, the micropore resistance is also shown to be larger than that of CFN450. This can be attributed to the fact that the removal of surface oxides upon calcination reduced the surface polarity and thus the wettability of the carbons in aqueous solutions.

The stability of the prepared capacitors can be examined by conducting repeated charge-discharge cycling. A capacitor equipped with CFN450 electrodes was charged and discharged between 0 and 0.6 V at 3 mA to confirm the stability. The variations of the discharge capacitance and coulombic efficiency[33] with cycle number are shown in Fig. 9. The results exhibit that the capacitor has stable capacitance (about 166 $F\ g^{-1}$) and coulombic efficiency (about 99.5%) over 100 cycles.

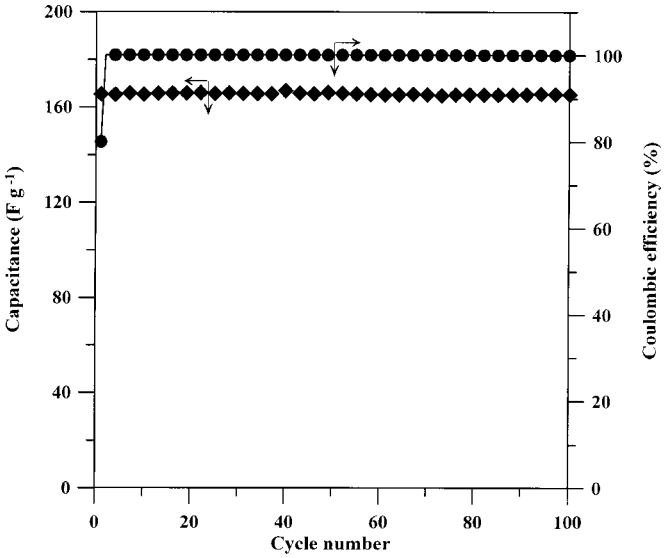

Figure 9. Variation of capacitance and coulombic efficiency with cycle number for the CFN450 electrode (2 cm^2) charged and discharged at 3 mA in 1 M H_2SO_4.

Conclusions

Oxidation through nitric acid treatment was found to enhance the electrochemical capacitance of PAN-based activated carbon fabric electrodes in H_2SO_4 solution. The capacitance enhancement can be attributed to the increase in the population of the CO-desorbing complexes, while the CO_2-desorbing complexes show a negative effect in double-layer formation. Upon heat-treating the oxidized carbon fabric at 450°C, most the CO_2-desorbing complexes were removed while the population of CO-desorbing complexes reached a maximum. This treatment has produced electrodes with the highest capacitance from the oxidized fabric.

Cyclic voltammetry showed that the presence of the CO-desorbing complexes significantly enhanced the double-layer formation and thus the capacitance. This indicates that due to the local changes of electronic charge density a proton adsorbed by a carbonyl or quinone-type site facilitates an excess specific double-layer capacitance. The faradaic current increased with the total number of oxygen atoms on the surface, indicating that both the CO- and CO_2-desorbing complexes enhanced the redox process.

Charge-discharge cycling experiments showed that the capacitance decreased slightly with the discharge current, indicating a low ohmic resistance in carbon micropores due to the small pore depth. Equivalent circuit analysis on the ac impedance results showed that the total resistance of the capacitors was mainly attributed to the electrical connection resistance between the fabric and the backing plate as well as that between the fibers. The connection resistance was found to increase upon the introduction of surface oxides. The carbon electrode that had been calcined at 450°C exhibited the smallest overall resistance because of its negligibly small micropore resistance.

Due to the treatment of nitric acid oxidation followed by appropriate calcination, the overall specific capacitance was found to increase more than 40% (*e.g.*, from 120 to 170 $F\ g^{-1}$) while the IR drop remained unchanged. The capacitors prepared in the present work exhibit excellent capacitance stability with a coulombic efficiency of 99.5% over 100 cycles.

Acknowledgments

Financial support from the National Science Council of Taiwan is gratefully acknowledged, project no. NSC 90-2214-E-006-008.

National Cheng Kung University assisted in meeting the publication costs of this article.

References

1. R. Kötz and M. Carlen, *Electrochim. Acta*, **45**, 2483 (2000).
2. M. Ishikawa, M. Ihara, M. Morita, and Y. Matsuda, *Electrochim. Acta*, **40**, 2217 (1995).
3. Y. Matsuda, K. Inoue, H. Takeuchi, and Y. Okuhama, *Solid State Ionics*, **113-115**, 103 (1998).
4. L. Bonnefoi, P. Simon, J. F. Fauvarque, C. Sarrazin, and A. Dugast, *J. Power Sources*, **79**, 37 (1999).
5. T.-C. Weng and H. Teng, *J. Electrochem. Soc.*, **148**, A368 (2001).
6. H. Shi, *Electrochim. Acta*, **41**, 1633 (1996).
7. I. Tanahashi, A. Yoshida, and A. Nishino, *J. Electrochem. Soc.*, **137**, 3052 (1990).
8. T. Nagaoka and T. Yoshino, *Anal. Chem.*, **58**, 1037 (1986).
9. T. Nagaoka, T. Fukunaga, T. Yoshino, I. Watanabe, T. Nakayama, and S. Okazaki, *Anal. Chem.*, **60**, 2766 (1988).
10. J. M. Miller, B. Dunn, T. D. Tran, and R. W. Pekala, *J. Electrochem. Soc.*, **144**, L309 (1997).
11. A. Nakamura, T. Inui, N. Kinomura, and T. Suzuki, *Carbon*, **38**, 1361 (2000).
12. F. Adib, A. Bagreev, and T. Bandosz, *Langmuir*, **16**, 1980 (2000).
13. K. Kinoshita, *Carbon: Electrochemical and Physicochemical Properties*, p. 302, John Wiley & Sons, New York (1988).

14. R. L. McCreery, K. K. Cline, C. A. McDermott, and M. T. McDermott, *Colloids Surf., A*, **93**, 211 (1994).
15. T. Momma, X. Liu, T. Osaka, Y. Ushio, and Y. Sawada, *J. Power Sources*, **60**, 249 (1996).
16. B. E. Conway, *Electrochemical Supercapacitors*, p. 259, Kluwer Academic/Plenum Publishers, New York (1999).
17. J. Koresh and A. Soffer, *J. Electrochem. Soc.*, **124**, 1379 (1977).
18. J. S. Noh and J. A. Schwarz, *Carbon*, **28**, 675 (1990).
19. S. S. Barton, M. J. B. Evans, E. Halliop, and J. A. F. MacDonald, *Carbon*, **35**, 1361 (1997).
20. Y. Otake and R. G. Jenkins, *Carbon*, **31**, 109 (1993).
21. L. R. Radovic and C. Sudhakar, in *Introduction to Carbon Technologies*, H. Marsh, E. A. Heintz, and F. Rodríguez-Reinoso, Editors, p. 103, University of Alicante, Alicante, Spain (1997).
22. S. Lowell and J. E. Shields, *Powder Surface Area and Porosity*, 3rd ed., Chapman & Hall, New York (1991).
23. F. Rodríguez-Reinoso, M. Molina-Sabio, and M. T. González, *Carbon*, **33**, 15 (1995).
24. C. Moreno-Castilla, J. Rivera-Utrilla, J. P. Joly, M. V. López-Ramón, M. A. Ferro-García, and F. Carrasco-Marín, *Carbon*, **33**, 1417 (1995).
25. X. Liu and T. Osaka, *J. Electrochem. Soc.*, **144**, 3066 (1997).
26. S. Yoon, J. Lee, T. Hyeon, and S. M. Oh, *J. Electrochem. Soc.*, **147**, 2507 (2000).
27. R. W. Couglin and F. S. Ezra, *Environ. Sci. Technol.*, **2**, 291 (1968).
28. T. Asakawa and K. Ogino, *J. Colloid Interface Sci.*, **102**, 348 (1984).
29. R. de Levie, *Electrochim. Acta*, **8**, 751 (1963).
30. L. G. Austin and E. G. Gagnon, *J. Electrochem. Soc.*, **120**, 251 (1973).
31. J. R. Miller, in *Electrochemical Capacitors*, F. M. Delnick and M. Tomkiewicz, Editors, PV 95-29, p. 246, The Electrochemical Society Proceedings Series, Pennington, NJ (1996).
32. E. Gileadi, *Electrode Kinetics*, p. 222, VCH Publishers, New York (1993).
33. T. Osaka, X. Liu, M. Nojima, and T. Momma, *J. Electrochem. Soc.*, **146**, 1724 (1999).